P H Y S I C A L   R E V I E W   L E T T E R S

Charge Transfer Doping of Silicon

K. J. Rietwyk,[1,*] Y. Smets,[1] M. Bashouti,[2,3] S. H. Christiansen,[3] A. Schenk,[1] A. Tadich,[4] M. T. Edmonds,[5]
J. Ristein,[6] L. Ley,[1,6] and C. I. Pakes[1,†]

[1]*Department of Physics, La Trobe University, Victoria 3086, Australia*
[2]*Max-Planck-Institute for the Science of Light, D-91058 Erlangen, Germany*
[3]*Institute of Nanoarchitectures for solar energy conversion, Helmholtz-Centre Berlin (HZB), D-14109 Berlin, Germany*
[4]*Australian Synchrotron, 800 Blackburn Road, Clayton, Victoria 3168, Australia.*
[5]*School of Physics, Monash University, Clayton, Victoria 3800, Australia*
[6]*Technische Physik, Universität Erlangen, D-91058 Erlangen, Germany*
(Received 4 December 2013; published 18 April 2014)

We demonstrate a novel doping mechanism of silicon, namely *n*-type transfer doping by adsorbed organic cobaltocene ($CoCp_{2*}$) molecules. The amount of transferred charge as a function of coverage is monitored by following the ensuing band bending via surface sensitive core-level photoelectron spectroscopy. The concomitant loss of electrons in the $CoCp_{2*}$ adlayer is quantified by the relative intensities of chemically shifted Co2p components in core-level photoelectron spectroscopy which correspond to charged and neutral molecules. Using a previously developed model for transfer doping, the evolution in relative intensities of the two components as a function of coverage has been reproduced successfully. A single, molecule-specific parameter, the negative donor energy of $-(0.50 \pm 0.15)$ eV suffices to describe the self-limiting doping process with a maximum areal density of transferred electrons of 2×10^{13} cm^{-2} in agreement with the measured downward band bending. The advantage of this doping mechanism over conventional doping for nanostructures is addressed.

The scaling of silicon-based electronics to smaller dimensions over the last 50 years has shifted the focus of device design from bulk to surface and interface properties. [1] This has culminated in the last decade in the synthesis of Si-nanowires (NW) and their emerging application in photovoltaics [2] and sensors [3]. As with conventional electronics, these applications rely on the possibility to dope Si locally *n*- and *p*-type and the approach taken is the usual one, namely the introduction of substitutional donors and acceptors. The dopants may be already present in the substrate material and remain so in the NW yielding axial p-n junctions [4], or may be introduced either during growth of the NW [5–7] or post growth by ion implantation, for example. [8] In either case, a subsequent activation anneal is of the essence. While these methods have led to encouraging initial device performances so far, there are issues with this approach that are necessarily connected with the nanometer dimensions of the devices. For volumes in the range of $(10 \text{ nm})^3$ the number of dopant atoms is a mere 10 on average for typical doping concentrations of 10^{19} cm^{-3}. Hence, on statistical grounds, one expects a non-negligible variation in the actual carrier concentration in the nm-size devices. In addition, it has been suggested that due to the dielectric mismatch between silicon and its surrounding in a surface sheath of the order of the dopant Bohr radius (~ 6 nm for a typical donor) the screening of the dopant Coulomb potential is insufficient to lower the ionization energy to

its bulk value. [9,10] As a consequence, dopant atoms in this sheath are effectively inactive and that leads to a reduction in the carrier concentration and an increase in resistance with diminishing NW diameter. [9,11] It is therefore of interest to explore alternative doping avenues that are free of these limitations.

One doping method that has enjoyed considerable success in the area of organic semiconductors is transfer doping whereby integer charges are transferred from one organic species to another. The propensity for spontaneous charge transfer requires the right disposition of empty and occupied electronic levels of the participating molecular species. If one were to apply this kind of doping to a conventional semiconductor an additional requirement would be the absence of surface or interface states that would otherwise accept the transferred charge preventing them from contributing to the free carriers of the semiconductor. To our knowledge, hydrogen terminated diamond is the only semiconductor where charge transfer to an adsorbed water layer [12] or to a strong molecular acceptor such as C_{60} and its fluorinated derivatives [13,14] has led to a substantial hole accumulation layer with its concomitant surface conductivity. In this case, the hydrogen termination passivates the surface by removing interfering surface states from the gap and at the same time lowers the ionization energy sufficiently to facilitate electron transfer from the valence band into the lowest unoccupied molecular orbital of the surface acceptor molecule. Here we

present what we believe to be the first report on n-type transfer doping of silicon. The molecular donor is decamethylcoboltocene (CoCp$_2$*) with an ionization energy and 3.3 eV for the condensed phase [15]. Silicon, by comparison has an electron affinity of about 4.0 eV which makes an electron transfer from CoCp$_2$* to Si thermodynamically possible, as we shall show below. The necessary passivation of the Si surface was achieved by alkylation and the resulting electron accumulation layer at the Si surface was quantified by the surface Fermi level shift and by the relative concentrations of positively charged and neutral donor molecules, respectively. Both pieces of information were obtained from core-level photoelectron spectroscopy (XPS).

The Si sample was a (111) oriented wafer with an effective bulk donor concentration of 10^{15} cm^{-3}. After the usual cleaning and HF etching procedure the surface was alkylated according to the process described in [16]. The alkylation results in a surface passivation and a certain protection against oxidation. The methyl terminated Si(111) surface is atomically flat [17] and exhibits a surface recombination velocity of ~20 cm s^{-1}, more than 20 times lower than that of the native silicon dioxide [18] attesting to an exceptionally low density of surface recombination centers. In air the surface oxidizes but the oxidation saturates at an oxide thickness corresponding to about 0.4 of a monolayer (ML) [19] which is, most importantly, not accompanied by an increase in surface recombination velocity. [18] The oxide saturated methyl terminated surface has therefore the electronic surface properties necessary for surface transfer doping and retains these properties for extended periods of time in air. The sample was utilized for the experiment about one month after alkylation. CoCp$_2$* was used as received from Aldrich [20].

Experiments were conducted in a three-chamber UHV system at the Australian Synchrotron. Initially, the sample was annealed to 175 °C for 1 hour *in vacuo* in order to remove physisorbed surface contaminants. The Si sample was then cooled to -70 °C and exposed to a CoCp$_2$* atmosphere of 10^{-8} mbar for 30 min. in order to establish an initial coverage with CoCp$_2$*. The low temperature is necessary because CoCp$_2$* sublimes at room temperature. After taking the initial photoelectron (PE) spectra also at -70 °C the sample was annealed for short periods of time at increasingly higher temperatures, re-cooled to -70 °C, and measured after each annealing step. In this way the evolution of the Fermi energy with CoCp$_2$* coverage could be established. The coverage of CoCp$_2$* after each annealing step was determined from the relative intensities of Si and Co core-level spectra using established PE attenuation models. PE spectra were taken at -70 °C using normal emission electron detection at photon energies which maximize surface sensitivity. The binding energy (BE) scale of all spectra is referenced to the Fermi level E_F of a gold sample in electrical contact with the sample by
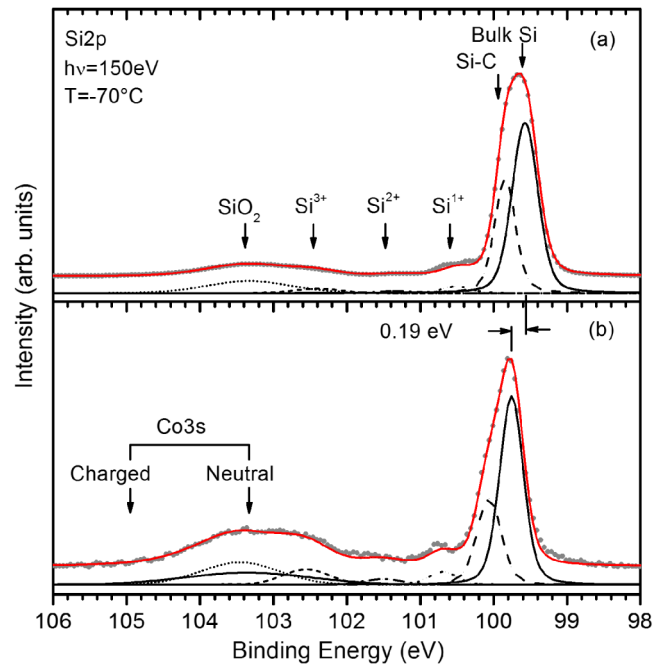

FIG. 1 (color online). Si2p core-level spectra taken at $h\nu = 150$ eV and $T = -70$ °C after annealing the surface at 175 °C (a) and subsequently exposing it for 30 min. to CoCp$_2$* at a pressure of 10^{-8} mbar (b). The Si2p$_{1/2}$ components have been removed from the data and the fits are offset for clarity.

establishing a Au4$f_{7/2}$ core-level BE of 84.00 eV. Relative core-level energies were determined by least squares fits with a precision of ± 0.05 eV. The accuracy of binding energies relative to E_F is ± 0.1 eV.

Fig. 1 shows the Si2p spectrum of the virgin surface (a) and after the deposition of three monolayers CoCp$_2$* (b) together with a deconvolution into component lines that were fitted to the data points after a Shirley background [21] correction. In order of increasing BE, the components in Fig. 1(a) correspond to bulk Si, Si bonded to the alkyl CH$_3$ group (Si-C), and to three Si suboxides (Si^{+n}, $n = 1, 2, 3$) plus SiO$_2$. The Si$_3$-Si-C chemical shift of 0.29 eV agrees with literature values that lie between 0.27 and 0.34 eV [19,22–24]. Analysis of the spectra (see supplemental Material [25]) suggest a monolayer termination with 45% oxide coverage, consistent with the literature. [19,22] The BE of the bulk Si2p$_{3/2}$ component is 99.57 eV rel. to E_F. Using the constant separation of 98.74 ± 0.10 eV between the bulk Si2p$_{3/2}$ peak and the VBM [28] and 1.12 eV for the band gap of silicon, the surface Fermi level position $E_C - E_F = 0.29$ eV is within the experimental accuracy of ± 0.14 eV compatible with the bulk Fermi level position at -70 °C, $(E_C - E_F)_{Bulk} = 0.17$ eV, for a bulk donor concentration of $N_D = 10^{15}$ cm^{-3}.

After CoCp$_2$* deposition (Fig. 1(b)) there are two changes. In the region of the SiO$_2$ component there is additional intensity which is ascribed to contributions from
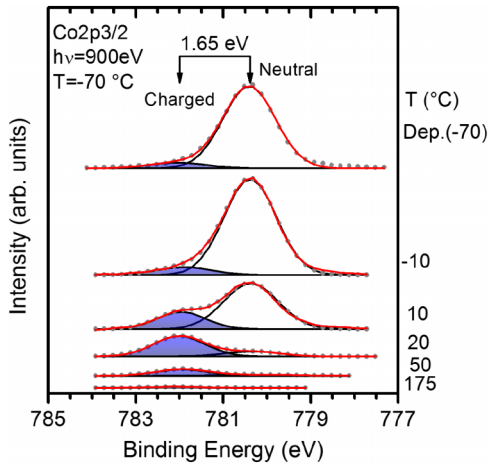
FIG. 2 (color online).   A selection of $Co2p_{3/2}$ core-level spectra taken at $h\nu = 900$ eV after a 30 min. deposition of $CoCp_2*$ at $-70\,°C$ and subsequent annealing steps. All spectra were measured at $-70\,°C$ and fitted with two components corresponding to charged (shaded) and neutral molecules.

the Co3s core-level of $CoCp_2*$. The position and intensity of this contribution were independently fixed by relating them to the non-interfering Co3p line at 42.1 eV lower BE, as measured in a wider energy scan (not shown). More importantly, however, is the overall shift of the Si2p spectrum by 0.19 eV towards higher BE relative to the bare sample which corresponds to an downward band bending by the same amount due to the accumulation of electrons transferred from $CoCp_2*$ to Si. Upon heating the surface to $-40\,°C$ the Si2p shifted a further 0.07 eV yielding a maximum shift of 0.26 eV. Subsequent anneals cause a reversal in the overall core-level shift.

Fig. 2 shows $Co2p_{3/2}$ spectra as a function of annealing temperature and hence decreasing $CoCp_2*$ coverage. The $Co2p_{3/2}$ line (and for that matter all other Co core-levels) consists of two components separated in energy by 1.65 eV with the higher BE component increasing in relative intensity with decreasing $CoCp_2*$ coverage. We ascribe this latter component to positively charged and the former to neutral cobaltocene. The positive charge is the result of integer charge transfer to Si and the changing intensity ratio indicates that charge transfer becomes less efficient with increasing coverage. The charged/uncharged interpretation of the two component core-level spectrum has previously been put forward for $CoCp_2^*$ on graphite surfaces [29], co-deposited with 2′,4′,6′-Trihydroxyacetophenone monohydrate (THAP) [30], and intercalated into SnS_2 single

crystals [31]. The double peak structure, together with the Si2p core-level shift, is thus the experimental signature of n-type transfer doping of Si by $CoCp_2*$.

We now turn to a more quantitative interpretation of the data. The model is based on the thermodynamic equilibrium between substrate and overlayer in the sense that the occupation of relevant electronic states is governed by a common Fermi level with the added proviso that there are no interface states, i.e., that the Schottky-Mott rule holds. This model has previously been applied successfully to the transfer doping of diamond [13,14] and the level alignment in organic–metal-oxide interfaces [32]. We further assume that charge exchange affects only the highest occupied molecular orbital (HOMO) of $CoCp_2*$ because other levels are far away on the scale of kT, and that charges are transferred as one elementary charge per molecule on account of a sizeable Coulomb energy which prevents multiple charging. Under these premises the probability P^+ that the normally fully occupied HOMO is occupied by a hole is given by

$$P^+ = \left[1 - \left(\exp\left(\frac{E_{HOMO} - E_F}{kT} \right) + 1 \right)^{-1} \right], \quad (1)$$

where E_{HOMO} and E_F are the HOMO and Fermi energies, respectively, and k, T have their usual meaning. A degeneracy g of the HOMO is equivalent to adding $kT \ln(g)$ to the Homo energy. It is convenient to rewrite Eq. (1) in terms of the substrate conduction band energy, $E_{HOMO} - E_F = E_{HOMO} - E_C + (E_C - E_F)$. The characteristic quantity for a particular combination of substrate and donor molecule is the "donor energy" Δ_0, which we define in analogy to bulk donors as, $\Delta_0 = (E_C - E_{HOMO})_0$, where the subscript "0" indicates the limit of vanishing coverage. As charge is transferred between donor and substrate the corresponding areal charges Q^+ on $CoCp_2*$ and $Q^- = -Q^+$ in Si are spatially separated and hence a dipole potential difference $\Delta\phi(Q)$ develops across the interface such that all energy levels of $CoCp_2*$ are lowered by $\Delta\phi$ relative to E_C. As a consequence, $E_C - E_{HOMO} = (E_C - E_{HOMO})_0 + \Delta\phi = \Delta_0 + \Delta\phi$. Simultaneously, the negative charge Q^- induces a downward band bending in Si characterized by the surface potential $qV_0(Q)$ such that at the interface $(E_C - E_F) = (E_C - E_F)_{Bulk} - qV_0$. With these considerations and using Eq. (1), the following equation for the transferred areal charge density Q is obtained,

$$Q = qNP^+ = qN \left[1 - \left(\exp\left(\frac{(E_C - E_F)_{Bulk} - \Delta_0 - \Delta\phi(Q) - qV_0(Q)}{kT} \right) + 1 \right)^{-1} \right], \quad (2)$$

where N is the areal density of donor molecules and q the elementary charge.

The connection between extra electron charge Q^- in Si and the surface potential $qV_0(Q)$ is calculated by solving Poisson's equation according to [33] and is given by

$$Q^- = \sqrt{2\varepsilon\varepsilon_0 kTN_D}\sqrt{\exp\left(\frac{qV_0}{kT}\right) - \frac{qV_0}{kT} - 1}, \quad (3)$$

where N_D is the bulk donor concentration, and $\varepsilon\varepsilon_0 = 11.9\varepsilon_0$ is the permittivity of Si. This is, of course, the equation that governs the accumulation regime of a channel Si-MOSFET as well.

The dipole potential $\Delta\Phi$ is given by the electric field F emerging from the Si accumulation layer multiplied by the distance d between Si surface and the counter charge in the cobaltocene layer $\Delta\Phi = eF_i d = eQd/(\varepsilon_i\varepsilon_0)$ where F_i and ε_i are the field and permittivity in the interface region, respectively. This expression, incidentally, is identical to that of the capacitor model that has been shown to work very well for insulating surfaces [14,32]; that is, $\Delta\phi = eQ/C_\square$ where $C_\square = \varepsilon_i\varepsilon_0/d$ is the interface capacitance per unit area. Taking for the distance d the length of the Si-C bond (1.9 Å) plus the CH_3 surface termination (0.37 Å) and half the thickness of a molecule lying flat on the surface (2.5 Å) yields an estimate of 4.8 Å for d. For ε_i we adopt a value of 3.6 based on the fits of the experimental data as discussed later.

With this approximation we have evaluated Eq. (3) at $T = -70\,°C$, and the result for P^+ is plotted as the solid line in Fig. 3(a) as a function of $CoCp_2*$ coverage. P^+ is interpreted as the doping efficiency, i.e., the number of positively charged molecules divided by their total number. This quantity is equal to the intensity ratio of the higher BE $Co2p_{3/2}$ component to the total $2p_{3/2}$ intensity in Fig. 2 and is also plotted in Fig. 3 as solid dots. The best agreement between the model and data is obtained for $\varepsilon_i = 3.6$ and

$\Delta_0 = -0.50$ eV, i.e., an initial HOMO energy above the conduction band minimum of Si. Hence, the doping efficiency is unity at the beginning and rapidly drops to values close to zero as the coverage increases. The latter is a consequence of the dipole potential and the band bending which both tend to lower E_{HOMO} relative to E_F and hence reduce the probability for hole occupation of the HOMO as the amount of transferred charge increases.

The areal electron density Q in silicon is given by the integral over the incremental coverages weighted by the doping efficiency P^+. In Fig. 3(b) a plot of Q calculated with the same parameters as before is given along with the corresponding experimental data as a function of $CoCp_2*$ coverage. Both track each other as well as can be expected and the maximum charge transfer equals 2×10^{13} cm^{-2} and that is essentially reached at a cobaltocene coverage of one monolayer. An independent value for the charge density can also be determined from the band bending qV_0 using Eq. (3), from which a maximum density of 3×10^{13} cm^{-2} is obtained. However, the latter method exhibits a much large uncertainty in a charge density. See Supplemental Material [25] for a comparison of the uncertainties.

The best agreement between experimental data and our model in both Fig. 3(a) and 3(b) holds for $\Delta_0 = -0.50$ eV and an interface dielectric constant $\varepsilon_i = 3.6$, a value only slightly larger than the 3.0 measured for $CoCp_2*$ [34]. Fits still compatible with the experimental errors are obtained when ε_i is varied by ± 1 unit and Δ_0 by ± 0.15 eV

The initial donor energy $\Delta_0 = (E_C - E_{HOMO})_0$ in the framework of the Schottky-Mott rule is given by the energy difference between the electron affinity of the Si surface and the ionization energy of $CoCp_2*$, $\Delta_0 = \chi_{Si} - IE_{CoCp2*}$. The electron affinity of the $-CH_3$ and oxide terminated Si(111) surfaces are 3.68 eV [22] and 4.05 [35], respectively; taking the average of these weighted by the relative alkyl and
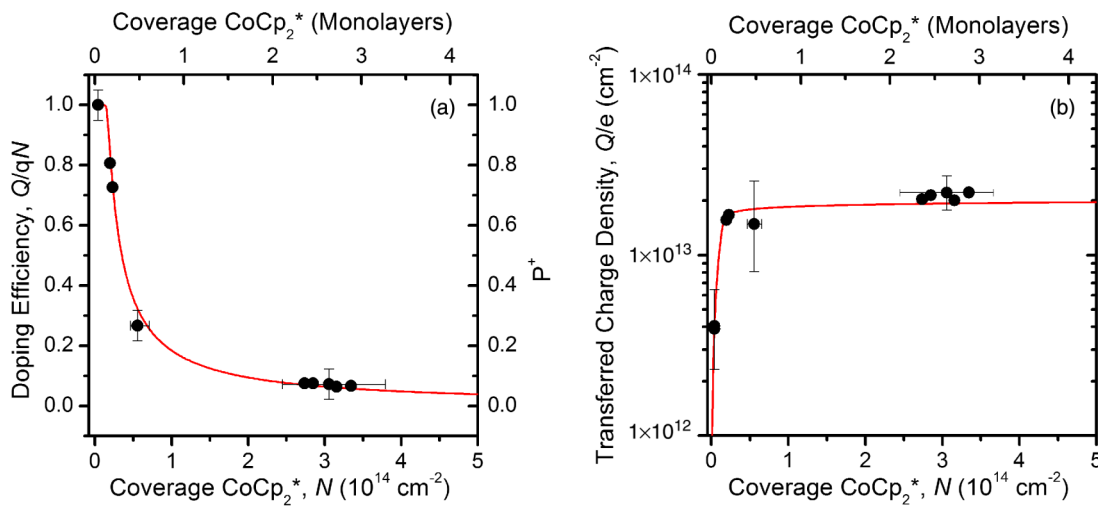

FIG. 3 (color online). (a) Experimentally determined doping efficiency Q/eN (data points) and the calculated probability P^+ of positive charge on a $CoCp_2*$ molecule (line) as a function of coverage. (b) Total transferred charge density from the data (data points) and as derived (line) by integrating the curve in Fig. 3(a). Both calculated curves are derived for a donor energy of $\Delta_0 = -0.50$ eV and $\varepsilon_i = 3.6$.

oxide coverages as determined above, the electron affinity of the surface is estimated to be 3.8 eV. The ionization energy of $CoCp_2*$ in the condensed phase is 3.30 eV [15] yielding $\Delta_0 = -0.50$ eV in perfect albeit likely fortuitous agreement with the experimentally derived value.

In summary, we have demonstrated the feasibility of transfer doping Si n-type by exposure to the organic donor molecule $CoCp_2*$. The maximum achievable electron density is about 2×10^{13} cm^{-2}, which is comparable to charge densities achieved in Si-based MOS transistors. The ease of doping which doesn't require any annealing step and allows for a ready adjustment of the transferred charge by controlling the coverage makes this type of doping a versatile and promising doping alternative for Si NW arrays or other Si-based nanostructures. Added benefits are as follows. The spatial separation of donor charges from the conducting channel is likely to improve the carrier mobility due to the reduction in ionized impurity scattering as also found in semiconductor heterostructures. The fact that the donor energy turns out to be negative means that the donating level lies above the Si conduction band. Hence, the doping process requires no activation energy as in conventional doping by substitutional donors. This renders this type of doping effective down to the lowest temperatures and carrier freeze-out will not be observed. Naturally, we do not claim that transfer doping requiring low temperatures is a viable alternative for real world applications but the results presented here provide a proof of concept. However, the formalism developed here to calculate the doping efficiency provides a tool to predict the efficiency of other potential donor molecules. After trivial modification, the same formalism can be applied to acceptor molecules for p-type doping as well and it is envisaged that eventually organically doped Si p-n junctions will be available.

[*]Corresponding author.
k.rietwyk@latrobe.edu.au
[†]c.pakes@latrobe.edu.au

[1] M. F. Bukhori, S. Roy, and A. Asenov, IEEE Trans. Electron Devices **57**, 795 (2010).
[2] A. I. Hochbaum, and P. Yang, Chem. Rev. **110**, 527 (2010).
[3] Y. Paska, T. Stelzner, O. Assad, U. Tisch, S. Christiansen, and H. Haick, ACS Nano **6**, 335 (2012).
[4] V. Sivakov, G. Andra, A. Gawlik, A. Berger, J. Plentz, F. Falk, and S. H. Christiansen, Nano Lett. **9**, 1549 (2009).
[5] B. Tian, X. Zheng, T. J. Kempa, Y. Fang, N. Yu, G. Yu, J. Huang, and C. M. Lieber, Nature (London) **449**, 885 (2007).
[6] E. C. Garnett, and P. Yang, J. Am. Chem. Soc. **130**, 9224 (2008).
[7] L. Tsakalakos, J. Balch, J. Fronheiser, B. A. Korevaar, O. Sulima, and J. Rand, Appl. Phys. Lett. **91**, 233117 (2007).
[8] P. Das Kanungo, R. Kogler, K. Nguyen-Duc, N. Zakharov, P. Werner, and U. Gosele, Nanotechnology **20**, 165706 (2009).
[9] M. T. Björk, H. Schmid, J. Knoch, H. Riel, and W. Riess, Nat. Nanotechnol. **4**, 103 (2009).
[10] M. Pierre, R. Wacquez, X. Jehl, M. Sanquer, M. Vinet, and O. Cueto, Nat. Nanotechnol. **5**, 133 (2009)
[11] M. Diarra, Y.-M. Niquet, C. Delerue, and G. Allan, Phys. Rev. B **75**, 045301 (2007).
[12] F. Maier, M. Riedel, B. Mantel, J. Ristein, and L. Ley, Phys. Rev. Lett. **85**, 3472 (2000).
[13] P. Strobel, M. Riedel, J. Ristein, and L. Ley, Nature (London) **430**, 439 (2004).
[14] M. T. Edmonds, M. Wanke, A. Tadich, H. M. Vulling, K. J. Rietwyk, P. L. Sharp, C. B. Stark, Y. Smets, A. Schenk, Q.-H. Wu, L. Ley, and C. I. Pakes, J. Chem. Phys. **136**, 124701 (2012).
[15] C. K. Chan, W. Zhao, S. Barlow, S. Marder, and A. Kahn, Org. Electron. **9**, 575 (2008)
[16] M. Y. Bashouti, T. Stelzner, S. Christiansen, and H. Haick, J. Phys. Chem. C **113**, 14823 (2009).
[17] H. Yu, L. J. Webb, R. S. Ries, S. D. Solares, W. A. Goddard III, J. R. Heath, and N. S. Lewis, J. Phys. Chem. B **109** 671 (2005).
[18] W. J. Royea, A. Juang, and N. S. Lewis, Appl. Phys. Lett. **77** 13 (2000).
[19] L. J. Webb, D. J. Michalak, J. S. Biteen, B. S. Brunschwig, A. S. Y. Chan, D. W. Knapp, H. M. Meyer, E. J. Nemanick, M. C Traub, and N. S. Lewis, J. Phys. Chem. B **110**, 23450 (2006).
[20] Sourced from Sigma-Aldrich, http://www.sigmaaldrich.com/catalog/product/aldrich/401781.
[21] D. A. Shirley, Phys. Rev. B **5**, 4709 (1972).
[22] R. Hunger, R. Fritsche, B. Jaeckel, W. Jaegermann, L. J. Webb, and N. S. Lewis, Phys. Rev. B **72**, 045317 (2005).
[23] J. Terry, M. R. Linford, C. Wigren, R. Cao, P. Pianetta, and C. E. D. Chidsey, J. Appl. Phys. **85**, 213 (1999)
[24] L. J. Webb, E. J. Nemanick, J. S. Biteen, D. W. Knapp, D. J. Michalak, M. C. Traub, A. S. Y. Chan, B. S. Brunschwig, and N. S. Lewis, J. Phys. Chem. B **109**, 3930 (2005).
[25] See Supplemental Material http://link.aps.org/supplemental/10.1103/PhysRevLett.112.155502, which includes Refs. [19,22,26,27].
[26] J. J. Yeh and I. Lindau, At. Data Nucl. Data Tables **32**, 1 (1985).
[27] S. Tanuma, C. J. Powell, and D. R. Penn, Surf. Interface Anal. **21**, 165 (1994).
[28] F. J. Himpsel, G. Hollinger, and R. A. Pollak, Phys. Rev. B **28**, 7014 (1983).
[29] O. Henrion and W. Jaegermann, Surf. Sci. **387**, L1073 (1997).
[30] C. K. Chan, A. Kahn, Q. Zhang, S. Barlow, and S. R. Marder, J. Appl. Phys. **102**, 014906 (2007).
[31] L. Hernan, J. Morales, L. Sanchez, J. Santos, J. P. Espinos, A. R. Gonzalez-Elipe, and J. P. Holgado, Surf. Sci. **477** L295 (2001).
[32] L. Ley, Y. Smets, C. I. Pakes, and J. Ristein, Adv. Funct. Mater. **23**, 794 (2013).
[33] H. Uebensee, Phys. Status Solidi B **147**, 823 (1988).
[34] M. A Gaffar and A. G. Hussien, J. Phys. Chem. Solids **62**, 2011 (2001).
[35] C. A. Hacker, Solid-State Electron. **54**, 1657 (2010).